ELSEVIER

Ceramics International 28 (2002) 515–520

CERAMICS INTERNATIONAL

www.elsevier.com/locate/ceramint

Development of glass-ceramics by sintering and crystallization of fine powders of calcium-magnesium-aluminosilicate glass

D.U. Tulyaganov[a], M.J. Ribeiro[b], J.A. Labrincha[a,*]

[a]*Ceramics and Glass Engineering Department UIMC, University of Aveiro, 3810-193 Aveiro, Portugal*
[b]*ESTG, Polytechnic Institute of Viana do Castelo, 4900 Viana do Castelo, Portugal*

Received 8 October 2001; received in revised form 9 December 2001; accepted 19 December 2001

Abstract

Natural raw materials normally used in the ceramic and glass industry were studied for the production of calcium–magnesium–aluminosilicate glass or glass-ceramic materials. Sintering and crystallization processes of fine powders of parent glass with chemical composition (wt.%) 46.00 SiO_2, 15.90 Al_2O_3, 1.20 Fe_2O_3, 0.42 TiO_2, 23.50 CaO, 9.37 MgO, 0.04 Na_2O, 0.98 K_2O, 1.95 P_2O_5 and 0.35 CaF_2 were studied. Crystallization kinetics of glass-ceramics was carefully examined by DTA, XRD, and SEM techniques and by dilatometric studies. The desired sequence of events, i.e. nucleation, sintering and devitrification occurred by heat-treating the glassy powder. However, crystallization of the parent glass did not follow phase diagram predictions, since anomalous appearance of akermanite phase was detected along with expected anorthite and diopside precipitation. A reasonable explanation for this unexpected observation is given.

Keywords: A. Sintering; D. Glass ceramics; D. Silicates; Ca–Mg–Al

1. Introduction

Glass-ceramics are normally obtained by a controlled crystallization process of suitable glasses. Internally or externally nucleation is promoted to develop micro-heterogeneities from which crystallization can subsequently begin. As a result, the amorphous reservoir of the parent glass transforms into a uniform microcrystalline ceramic. The composition of the crystalline phases and the crystallite sizes define the properties of the final material. Therefore, the major components and the composition of parent glass are selected to ensure precipitation of crystals that provide desired properties on a glass-ceramic [1–4].

In the case of internally nucleated glass-ceramics, the use of high specific surface glass-powders will act as uniformly scattered nuclei and no addition of a special nucleating agent is required. Subsequently densification of the glass-powder compact must take place prior to devitrification. This sequence of events starting near the end of the sintering stage comes before crystallization starts which allows dense materials to be obtained [5,6].

Other relevant aspects of the development of glass-ceramic materials include environmental and economical issues. The use of cheap and abundant raw materials as glass batch constituents is logically preferred [7–9]. In our previous work, a cross-section join in the glass-forming region of the fluorapatite–anorthite–diopside ternary system that corresponds to a constant fluorapatite (4.8 wt.%) content, was selected for the determination of the base glass compositions [10]. The range of base glass compositions, in which diopside and anorthite phases are able to precipitate during heat treatment, was then established. Such type of glasses tends to show easy surface crystallization. Sintering and crystallization behaviour of glass-powder with the nominal composition (wt.%) 47.31 SiO_2, 15.71 Al_2O_3, 24.24 CaO, 9.66 MgO, 2.01 P_2O_5 and 0.37 CaF_2 has been carefully studied. The aim to reproduce, as close as possible, the alkali-free glass composition by using natural sedimentary rocks as starting materials has been attempted. As major changes, about 0.5% of alkali oxides and slightly more than 0.6% of Fe_2O_3 were incorporated with natural raw materials. A frit was obtained by melting at 1350–1380°C. Different shaped samples were then obtained by low-pressure injection moulding followed by suitable de-bonding, sintering and crystallization steps. The formation of two crystalline

* Corresponding author. Tel.: +351-2343-70250; fax: +351-2344-25300.
E-mail address: jal@cv.ua.pt (J.A. Labrincha).

0272-8842/02/$22.00
PII: S0272-8842(02)00004-4

phases, anorthite and diopside, was obtained after heat treatment in the temperature interval 850–950 °C. The high wear resistance of these glass-ceramics permit their use as thread carriers in textile machines.

The present investigation aims to extend the crystallization study of the glass with the same nominal composition, to consider the wide variance in the chemical composition of natural raw materials now used. Their influence on crystallization kinetics is carefully examined.

2. Experimental procedure

Natural Portuguese raw materials normally used in the ceramic and glass industry were tested as starting materials for the parent glass formation. Ball clay (BM-8, Barracão- Leiria), dolomite (Barracão- Leiria), calcite (Parapedra, Rio Maior), and quartz sand (Mibal, Barqueiros-Barcelos) constituted the main components of the glass batch formulation. Reactive-grade $(NH_4)\cdot 2HPO_4$ and CaF_2 materials were used as a source of phosphorous pentoxide and fluoride, respectively. The chemical composition of the glass batch, calculated from the chemical composition of the raw materials, was as follows (wt.%): 46.00 SiO_2, 15.90 Al_2O_3, 1.20 Fe_2O_3, 0.42 TiO_2, 23.50 CaO, 9.37 MgO, 0.04 Na_2O, 0.98 K_2O, 1.95 P_2O_5, and 0.35 CaF_2. The deviation from the nominal composition of the glass was higher than in the previous investigation [10]. The content of alkaline oxides is slightly higher than 1%, while the ferric oxide content reaches 1.2%, i.e. about double that in the first study.

Quartz sand, dolomite, calcite and ball clay were separately dry ball milled. The mixture was melted in corundum crucibles by electrical means at 1400–1420 °C for 1 h. A frit was obtained by quenching through water at room temperature. Frit grains were dried and then milled in a high-speed porcelain ball mill. Glassy powders with specific surface areas (BET) of 2.7 (named GC-1) and 4.5 m^2/g (named GC-2) were obtained after 3 and 6 h milling, respectively. Glass properties characterisation was conducted with cast samples onto stainless steel moulds, at room temperature and without any annealing treatment.

Differential thermal analysis (DTA) was performed in a Rigaku Thermoflex apparatus up to 1000 °C and at a heating rate of 10 °C/min. Thermal expansion behaviour of the as-cast glass and crystallized samples was studied by dilatometric analysis performed at a heating rate of 10 °C/min (Netzsch 402 EP) and up to 1000 °C. An understanding of the thermal behaviour was crucial to define suitable crystallization firing schedules. Pressed rectangular bars (200 MPa) of about 4×5×50 mm obtained from humidified (3–5% water) glass powders were used. Samples were held at 700 °C for 1 h, after being heated at a constant rate of 10 °C/min. Then, the development of crystals was attempted by heat treatment in the region where crystallization peaks occurs (850, 880 and 920 °C for 1 h). Cooling to room temperature was carried out during 1.5 h.

Crystalline phases were identified by XRD in the 5–80° 2θ range using Cu-tube difractometer (Philips X′PERT, PW3040). Microstructural details were obtained by scanning electron microscopy (SEM-Jeol 5800 LV) on previously polished and etched (by dipping for 2 min in a 5 vol.% HF solution) glass-ceramic samples. Flexural strength of the glass-ceramic samples was determined using three-point bending test (Lloyd Instruments LR30K) on rectangular bars (3×4×40 mm). Apparent density of glass and glass-ceramic samples was determined by the Archimedes method (Hg immersion). Electrical specific resistance of glass-ceramic samples was measured by 2-probe impedance spectroscopy (HP 4284A potentiostat) on Pt-electroded samples.

3. Results and discussion

3.1. Property changes upon sintering and crystallization

Dilatometric analysis of the parent glass (Fig. 1) shows the transition temperature (T_g) at about 720 °C, while the softening point (T_s) is located around 760 °C. The nucleation temperature was selected as 700 °C, which is close to T_g.

Exothermic crystallization peaks are observed in DTA scans (Fig. 2). Glass powder with low specific surface area (2.7 m^2/g) shows two exothermic peaks of different magnitude: (i) a shallow one at 860 °C and (ii) one more intense and sharp at about 900 °C. By using finer powder glass particles (specific surface area of 4.5 m^2/g) the shallow peak is suppressed and one single deeper crystallization peak is observed. The higher number of nuclei in the finer material is responsible for the decreasing distance for crystalline growth [5] and explains the suppression of the first peak. In any case, temperatures between 850 and 900 °C were adopted as the suitable crystallization region.

Samples fired at 850, 880 and 920 °C are completely dense materials. Smoothing surface effects are due to

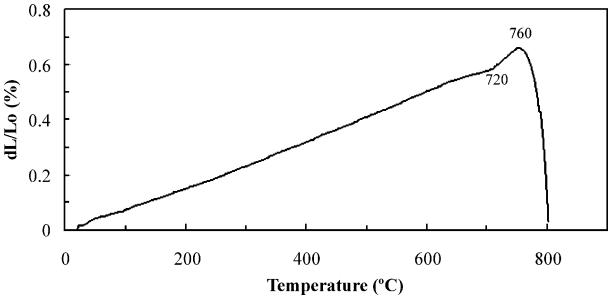

Fig. 1. Dilatometric curve of the parent glass, showing T_g and T_s points.

self-glazing. The use of lower firing temperatures (for example 800 °C) gives mechanically weak and highly porous materials. Table 1 shows the temperature evolution of some relevant properties of crystallized glasses. As it was expected, slightly higher shrinkage and density values are obtained for samples processed from finer glass-powders (GC-2). However, differences in mechanical strength are not so evident. The properties of each individual glass-ceramic do not significantly change with temperature (in the range 850–920 °C, i.e. the densification plateau), except the bending strength values that tend to increase with growing temperature. One possible explanation for this evolution is that the sintering process is practically complete at 850 °C and no significant densification effects are expected by further heating [6]. Mechanical reinforcement is achieved by the subsequent devitrification process.

Glass-ceramics possess moderate thermal expansion coefficients (see Table 2), varying between 77.3 and 82.7×10^{-7} °C^{-1}. These values are lower than that of the parent glass (86.5×10^{-7} °C^{-1}) and tend to decrease as crystallization proceeds (for higher temperatures and for the GC-2 glass). Fig. 3 shows dilatometric curves of glass-ceramics obtained from glass-powders of different specific surfaces areas. The behaviour of the coarser glass-powder samples is closer to the parent glass, especially that of the sample heat-treated at 850 °C. This confirms the lower devitrification intensity of GC-1 samples.

Arrhenius plots of the electrical resistivity of the parent glass and glass-ceramic materials are shown in Fig. 4.

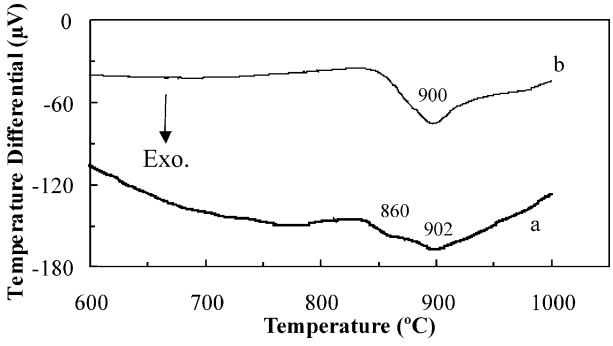

Fig. 2. DTA scans of the parent glass with different specific surface areas: (a) 2.7 m^2/g; (b) 4.5 m^2/g.

These values were obtained from impedance spectroscopy measurements, as shown in Fig. 5. Typically, the response of each system involves one single incomplete arc that reaches the origin, and tends to be highly depressed against the Z' axes as crystallization proceeds. All compositions are highly resistive and the response arc is not complete. High scattering results are obtained in the low frequency region and as a consequence, resistivity estimations by deconvolution of arcs are not very accurate, even if common mathematical routines

Table 2
Thermal expansion coefficient (CTE) of glass-ceramics samples fired at 850, 880 and 920 °C, determined between 20 and 600 °C

Temperature (°C)	CTE ($\times10^7$) °C^{-1}	
	GC-1	GC-2
850	82.7	79.4
880	80.7	78.3
920	78.4	77.3

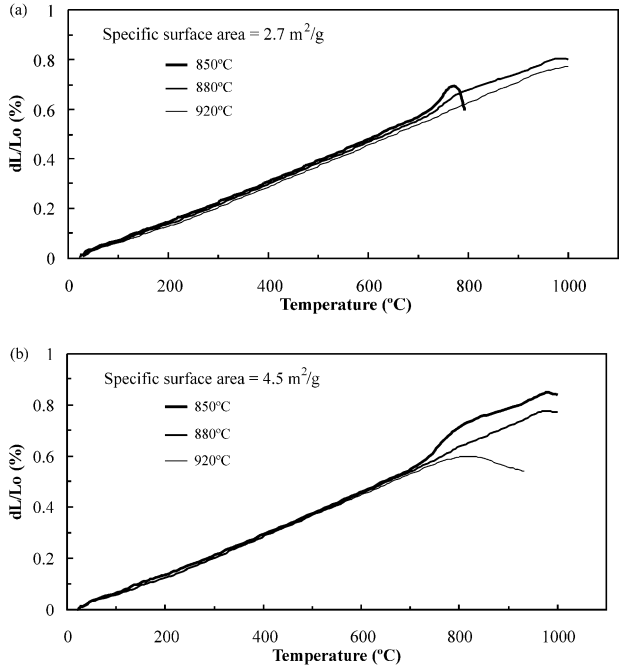

Fig. 3. Thermal expansion curves of glass-ceramics obtained from glass-powders (a) GC-1 and (b) GC-2, heat-treated at 850, 880 and 920 °C.

Table 1
Shrinkage, apparent density and flexural strength values of the crystallized glasses as a function of the temperature. Standard deviation values are given in parentheses

Properties	Shrinkage (%)		Density (kg/m^3)		Bending strength (MPa)	
Temperature (°C)	GC-1	GC-2	GC-1	GC-2	GC-1	GC-2
850	17.05 (±0.32)	17.90 (±0.14)	2760 (±6.8)	2790 (±12.4)	85.6 (±16.8)	91.8 (±3.6)
880	17.10 (±0.30)	17.90 (±0.18)	2760 (±29.8)	2780 (±3.5)	103.8 (±16.7)	94.7 (±13.5)
920	16.90 (±0.15)	18.10 (±0.32)	2750 (±19.2)	2770 (±17.4)	112.9 (±15.8)	111.6 (±14.5)

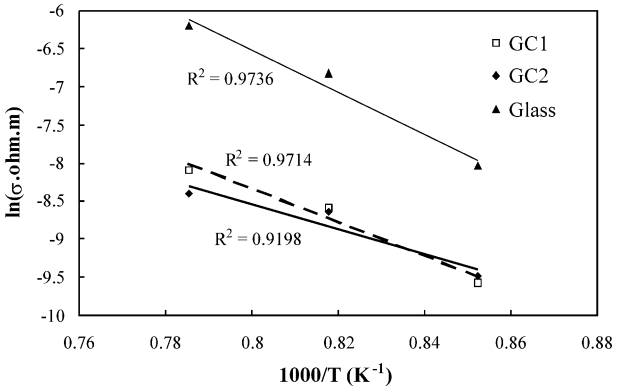

Fig. 4. Electrical specific resistivity of the parent glass and crystallized samples as a function of temperature (Arrhenius graphs).

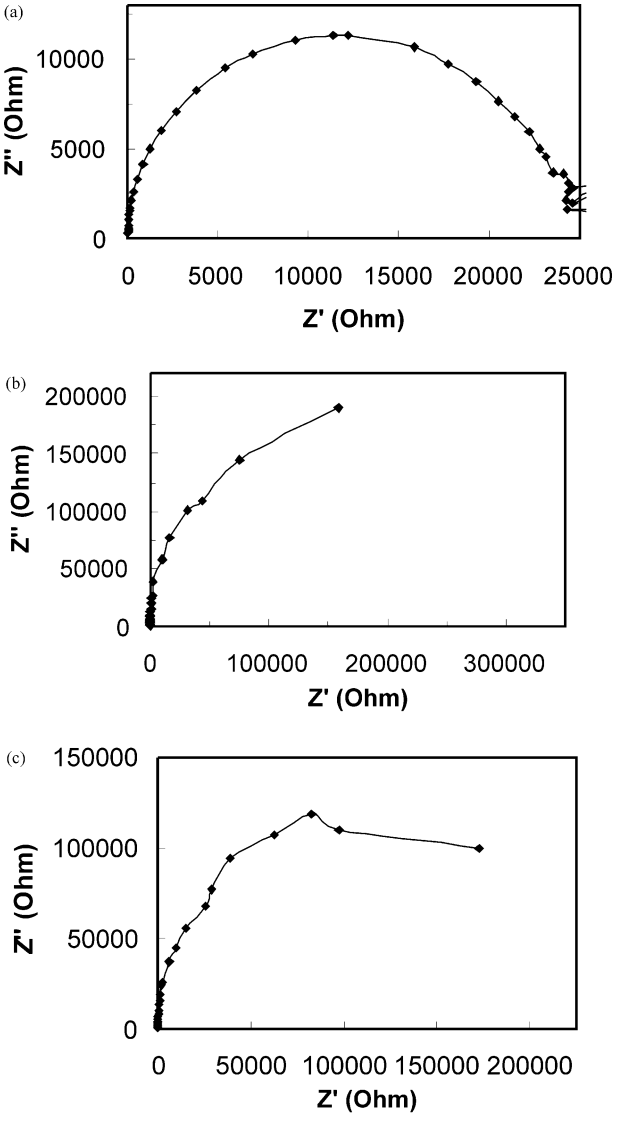

Fig. 5. Impedance spectra at 1000 °C for the parent glass (a), GC-1 (b), and GC-2 (c) samples.

[11] are used. At low temperatures (up to 850 °C) electrical behaviour is probably affected by the presence of pores (densification is not complete), being more evident for less compacted pressed samples (the parent glass is highly resistive). As a consequence, the GC-2 glass-ceramic sample shows higher conductivity values, despite the presence of crystals. Once the complete densification level (above 900 °C) is reached, the presence of crystalline phases is responsible for the higher electrical resistivity of the glass-ceramic samples. The increasing number of interfaces promoted by the crystallization process creates a highly discontinuous pathway for electrical transport carriers along the sample. The differences between GC-1 and GC-2 glass-ceramic samples are irrelevant, except at relatively low temperatures (850 °C) where the extent of crystallization or densification is somewhat different. The coarser GC-1 sample is less reactive and remaining pores are responsible for the lower conductivity value.

3.2. Structural and microstructural characterization

XRD results of glass-powder compacts heat-treated at 850, 880 and 920 °C suggest consecutive transformation of the parent glass into crystalline phases. Fig. 6 shows the evolution of the GC-1 sample. The degree of crystallinity of formed phases and the composition of the residual glass change with temperature evolution. The X-ray pattern of the sample obtained at 850 °C is still basically composed of an amorphous glassy phase and a few low intensity peaks of triclinic anorthite ($CaAl_2Si_2O_8$) are observed. A further temperature increase to 880 °C enhances the intensity of the anorthite peaks and weakly defined new phases of monoclinic diopside ($CaMgSi_2O_6$) and akermanite are observed. This phase relationship was unexpected, based on previous results obtained with a similar glass composition [10]. In the previous case, a lower amount of alkaline and iron oxides had been used, and only two

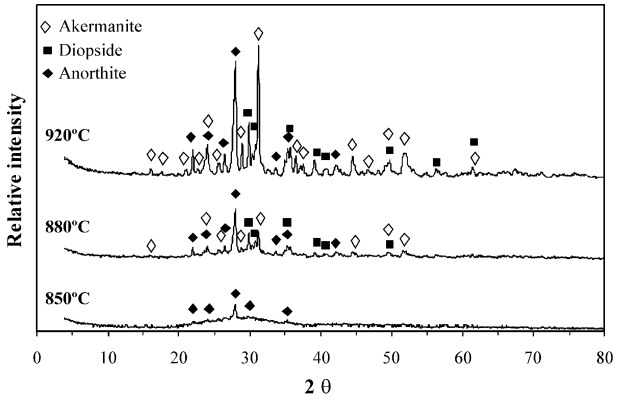

Fig. 6. X-ray diffraction patterns of the GC-1 glass-ceramic samples heat-treated at 850, 880 and 920 °C.

phases (anorthite and diopside) were found in the temperature region between 850 and 950 °C. The sample heat-treated at 920 °C still shows anorthite, diopside and akermanite as crystalline phases and the amount of residual glass is almost nil. In comparison to the other phases, akermanite peaks grow significantly in the temperature interval 880–920 °C, probably due to the presence of the mentioned impurities. Structural rearrangements might take place in the earlier stages of the crystallization process, ensuring the partial transformation of octahedrally into tetrahedrally coordinated magnesium, as will be detailed below. Furthermore, ghelenite ($Ca_2Al_2SiO_7$) and akermanite ($Ca_2MgSi_2O_7$) phases belong to the melilite group and have the same crystal structure [12,13], subsequently the X-ray peaks for both phases are coincident and it is difficult to process and identify each individual phase.

Fig. 7 shows representative microstructures of glass-ceramic GC-1 and GC-2 samples heat-treated at 920 °C. The GC-1 sample exhibits spherical and ellipsoid crystals of average size about 0.3–0.4 μm. Since the starting powder of the GC-2 material is even finer, its final microstructure involves smaller and randomly distributed crystals. The microstructure is more uniform and seems denser (Fig. 7B). In this case, is even more difficult to estimate the nature of the crystals, but according to XRD the observed particles should correspond to anorthite, akermanite and diopside.

3.3. Crystallization mechanism

According to Osborn [14] the binary anorthite-diopside system shows a single eutectic point at 1274 °C, corresponding to the compositional (wt.%) ratio 42:58. Along with the high temperature study in the fluorapatite–anorthite–diopside ternary system, the cross sectional join in the vicinity of the anorthite–diopside boundary corresponding to a constant amount of 4.8% fluorapatite was also studied [14]. The crystallization behaviour of glasses with composition 46.75–47.88 SiO_2; 13.96–17.45 Al_2O_3; 22.64–25.24 CaO; 8.78–10.54 MgO; 2.01 P_2O_5 and 0.37 CaF_2 (wt.%) was investigated [15]. Devitrification occurred according to phase diagram predictions, with anorthite and diopside being the main formed crystalline phases and fluorapatite the minor component. The use of natural raw materials did not cause significant differences despite the incorporation of alkaline (0.5%) and ferric (0.6%) oxides [15].

The same anorthite + diopside phase combination is expected in the present investigation. However, the devitrification process is somewhat different as a probable effect of the presence of higher amounts of alkaline oxides (slightly above than 1%), and Fe_2O_3 (about 1.2%), i.e. about double that in the previous work [15]. These impurities might modify the glass network by decreasing the relative proportion of bridging oxygen bonds to non-bridging oxygen bonds. As a result, the transformation of octahedral magnesium groups ($[MgO_6]^{10-}$) into tetrahedral groups ($[MgO_4]^{6-}$) and the deformation of $[SiO_3]^{2-}$ tetrahedral groups with the subsequent appearance of $[Si_2O_7]^{6-}$ diortogroups might occur. Magnesium tetrahedral groups would favour the crystallization of the end-member phase of the melilite group, akermanite. At the same time, the remaining octahedrons tend to be combined with $[CaO_6]^{10-}$ octahedrons and endless $[SiO_3]^{2-}$ groups, leading to diopside formation [16].

The probable sequence of events during glass powder heat-treatment is as follows: (i) near the glass transition temperature (T_g), the parent glass fine particles will act as uniformly scattered nuclei; (ii) further heating lead to a decrease in the viscosity of the batch and promotes densification by viscous coalescence; (iii) around 850 °C crystallization starts, resulting in the precipitation of

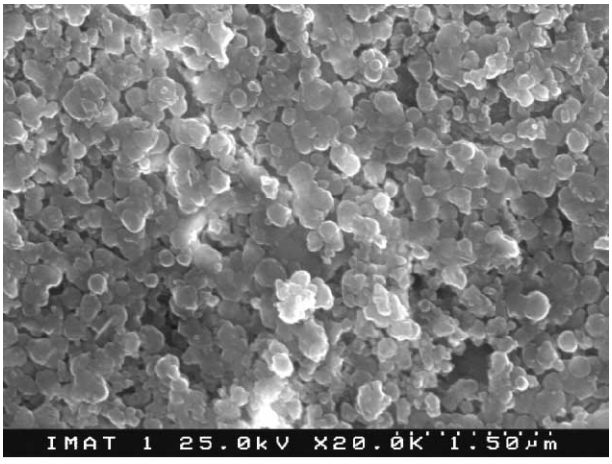

(a)

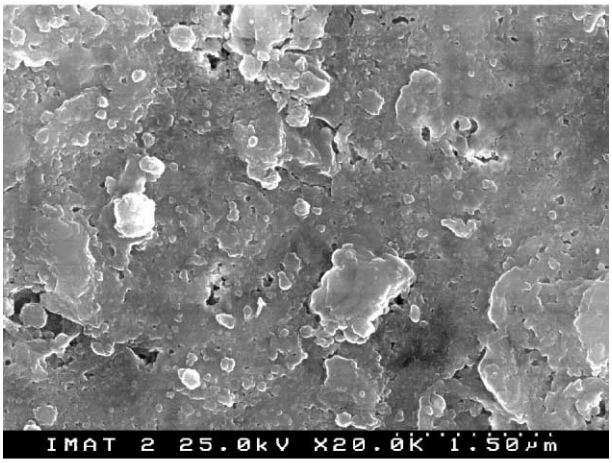

(b)

Fig. 7. SEM observations of (a) GC-1 and (b) GC-2 glass ceramic samples heat-treated at 920 °C.

anorthite. Increasing temperature will improve the degree of crystallinity and densification, and a fully dense glass-ceramic material composed of anorthite, akermanite and diopside crystals plus some residual glassy phase is formed.

4. Conclusions

Sintering and crystallization processes of the parent glass 46.00 SiO_2, 15.90 Al_2O_3, 1.20 Fe_2O_3, 0.42 TiO_2, 23.50 CaO, 9.37 MgO, 0.04 Na_2O, 0.98 K_2O, 1.95 P_2O_5 and 0.35 CaF_2 (wt.%), made from natural raw materials normally used for ceramics and glass fabrication were studied. Expected anorthite and diopside phases are present along with the unpredicted presence of akermanite crystals. This unusual crystallization behaviour was related to the presence of relatively high amounts of alkaline and ferric oxides.

The use of finer starting glass powders gives glass-ceramic materials with highly homogeneous microstructures and smoother surfaces. The glossy aspect is also retained. Simultaneous improvement of functional properties like the mechanical resistance to abrasion and flexural stresses will make these materials very attractive for several applications (e.g. to the textile industry). The use of natural (and cheap) raw materials and their adaptability for fabrication by different techniques (injection moulding, isostatic pressing, etc.) helps to produce cost competitive and multi-shaped devices.

Acknowledgements

Financial support from FCT (Portuguese Science Foundation) is greatly appreciated.

References

[1] P.W. Mcmillan, (Ed.), Glass-Ceramics, Academic Press, London, 1964.
[2] G.H. Beall, Glass-ceramics: recent developments and applications, in: M. Weinberg (Ed.), Ceramic Transactions, Vol. 30, American Ceramic Society, Westerville, OH, 1993, pp. 241–266.
[3] N.M. Pavlushkin (Ed.), Principals of Glass-Ceramics Technology, 2nd edition. Stroiizdat, Moscow, 1979 (in Russian).
[4] Z. Strnad (Ed.), Glass-Ceramic Materials, Elsevier, Amsterdam, 1986.
[5] S.H. Knickerbocker, A.H. Kumar, L.W. Herron, Cordierite glass-ceramics for multilayer ceramic packaging, Am. Ceram. Soc. Bull. 72 (1993) 90–95.
[6] C. Siligardi, M.C. D'Arrigo, C. Leonelli, Sintering behavior of glass-ceramic frits, Am. Ceram. Soc. Bull 79 (2000) 88–93.
[7] R.C. Monteiro, M.M. Rolim, Preparation of glass-ceramics from Portuguese basalt, Ciência e Technologia dos Materiais 4 (1992) 7–11 (in Portuguese).
[8] M.L. Öveçoglu, B. Kuban, H. Ozer, Characterization and crystallization kinetics of a diopside-based glass-ceramic developed from glass industry raw materials, J. Eur. Ceram. Soc. 17 (1999) 957–962.
[9] R.H. Bryden, D.G. Goski, W.F. Caley, Lime-alumina-silica processing incorporating minerals, J. Eur. Ceram. Soc. 19 (1999) 1599–1604.
[10] D.U. Tulyaganov, A.A. Ismatov, Development and application of anorthite-diopside containing glass-ceramics, in: A. Varshneya, D. Bickford, P. Bihuniak (Eds.), Ceramic Transactions, Vol. 29, American Ceramic Society, Westerville, OH, 1993, pp. 221–224.
[11] B. Boukamp, A non-linear squares least fit procedure for analysis of immitance data of electrochemical systems, Solid State Ionics 20 (1986) 31–44.
[12] Powder diffraction file, card no 35–592, 1992, database edition, Joint Committee on Powder Diffraction Standards, Swathmore, PA, USA.
[13] M.L. Öveçoglu, Microstructural characterization and physical properties of a slag-based glass-ceramic crystallized at 950 and 1100 °C, J. Eur. Ceram. Soc. 18 (1998) 161–168.
[14] E.F. Osborn, The system wollastonite-diopside-anorthite, Am. J. Sci. 240 (1942) 751–758.
[15] D.U. Tulyaganov, Phase equilibrium in the flourapatite-anorthite-diopside system, J. Am. Ceram. Soc. 83 (2000) 3141–3146.
[16] L.A. Zhunina, M.I. Kuzmenkov, L.W. Yaglov (Eds.), Pyroxene Glass-ceramics, Belorussia Government University, Minsk, 1974. in Russian.